A Parabolic Equation Code for Downslope Propagation in a Wedge

John Boyle, ECE 576

December 6, 2012

Contents

1 Problem Statement

The project proposal included the following:

> **Project Proposal - ECE 576**
> Parabolic wave equations are used to solve range-dependent propagation models in ocean acoustics. Such a model was tested by Jensen and Tindle (1987)[1] in the calculation of mode propagation in a wedge.
>
> Following the methods of Jensen and Tindle, I will perform the following:
>
> **Develop Code**
>
> - **Apply the approximations used in the paper.** These include the Thomson-Chapman form of the parabolic equation, a reference wavenumber update algorithm, and a specialized source function.
> - **Derive a PE code by following methods in *Computational Ocean Acoustics*[2].**
>   The book contains an appendix "Recipe for Simple PE Code" that will be the basis for my code.
> - **Design a wedge to use in the code.** The environmental parameters given in the paper will be implemented in numerical matrices to create a computational grid.
> - **Examine upslope and downslope propagation.**
>
> **Test Results**
>
> - **Compare code results to published results.** These are the figures in Jensen and Tindle's paper.
> - **Compare results to other underwater acoustics code results, e.g. KRAKEN.** The solution, if correct should match solutions obtained through other methods such as wavenumber integration and coupled normal modes.
> - **Explore time-domain solutions.** The solutions of the PE code give the steady-state frequency response. Through Fourier Transforms of results in a fixed frequency bandwidth, a time-domain solution could be obtained.

I successfully developed a PE code, though not in the exact form used by Jensen and Tindle. With the addition of a error-correcting factor within the split-step marching algorithm, the code produces qualitatively correct results. A large portion of development time went

[1] Numerical modeling results for mode propagation in a wedge, F. B. Jensen and C. T. Tindle, J. Acoust. Soc. Am. 82, 211 (1987)

[2] Jensen, F. B. (2011). Computational ocean acoustics. New York: Springer Science+Business Media, LLC.

towards isolating and examining the error. Therefore, I performed only a brief examination of downslope propagation in a wedge.

Comparison of a preliminary result for downslope propagation to published results is included in this report. Upslope propagation was not examined and results were not compared with other ocean acoustics codes. Time domain solutions will be explored at a later time.

The structure of this report is as follows: a description of the code developed, a comparison of its results to a reference solution and a discussion of differences, and an examination of results for downslope propagation in a wedge.

2 PE Code Development

The numerical model used in the code was developed following the section, "Appendix 1: Recipe for Simple PE Code," in *Computational Ocean Acoustics* (COA). The recipe is presented below and it is followed by a description of every equation used in each step, and where multiple options were available, explains the reasoning for the choice of formulation.

The basic "recipe" that will be followed is:

1. Select Spatial Grid Size.
2. Create Computational Domain.
3. Add Environment Parameters.
4. Calculate Squared Index of Refraction.
5. Define Starting Field.
6. Choose Marching FFT Algorithm.
7. Choose Numerical Fourier Transform.

2.1 Select Spatial Grid Size

For an analytical source function such as the standard Gaussian, an upper bound on the grid size in z is

$$\Delta z \leq \frac{\lambda}{4}.$$

Grid size in r is given by $\Delta r = (2-5)\Delta z$ for shallow water and $\Delta r = (20-50)\Delta z$ for deep water.

2.2 Create Computational Domain

The computational domain is created to include the physical domain and an additional absorption layer to simulate a half-space below the bottom layer. It is recommended in COA that the absorption layer thickness (in z) be equal to one third the thickness of the physical domain. The treatment of absorption in the absorption layer will be explained in the squared Index of Refraction section.

2.3 Add Environmental Parameters

The environmental parameters density, absorption, and sound speed may be mapped onto matrices of the size of the computational domain. For example, the sound speed of a computational ocean of depth D/2 above a ocean bottom of D/2 could be modeled by creating a matrix of depth D where the upper half contains the sound speed of water and the lower the sound speed of rock or sediment. In a computing environment optimized for element-wise operations, such as MATLAB, it may be best to create entire matrices for sound speed, density and absorption. In other computer environments and languages, this may be best accomplished through functions describing the boundaries between features. In either case, the results will be directly applied to the calculation of the squared index of refraction.

2.4 Calculate Squared Index of Refraction

Density, absorption, and sound speed are included in the parabolic equation,

$$\frac{\partial \psi}{\partial r} = \frac{ik_0}{2}\left(n^2 - 1 + \frac{1}{k_0^2}\frac{\partial^2}{\partial z^2}\right)\psi \tag{1}$$

through the squared index of refraction, n^2.

Following section 6.5.4 of COA, density variations may be included in the PE solution by solving the PE for density reduced pressure, $\widetilde{\psi} = \psi/\sqrt{\rho}$. This is included in the code through the starting field,

$$\widetilde{\psi}(0, z) = \psi(0, z)/\sqrt{\rho(0, z)}.$$

Pressure, $\psi(r, z)$, is retrieved from the final numerical field solution by multiplying by $\sqrt{\rho(r, z)}$.

Density variations are included in the squared index of refraction by

$$\widetilde{n^2} = n^2 + \frac{1}{2k_0^2}\left[\frac{1}{\rho(r, z)}\frac{\partial^2 \rho(r, z)}{\partial z^2} - \frac{3}{2\rho(r, z)^2}\left(\frac{\partial \rho(r, z)}{\partial z}\right)^2\right]. \tag{2}$$

To avoid infinite derivatives at a density boundary, the function

$$\rho(z) = \frac{1}{2}(\rho_1 + \rho_2) + \frac{1}{2}(\rho_2 - \rho_1)\tanh\left(\frac{z - D_0}{L}\right) \tag{3}$$

smooths a boundary between layers of densities ρ_1 and ρ_2. L is chosen with $k_0 L = 2$ so that the smoothed boundary will be an accurate approximation of the real boundary. This expression may also be used to find an analytic expression for the derivatives in Eq. (2).

In the expression for squared index of refraction (2), n^2 on the right-hand-side is given by

$$n^2 \simeq \left(\frac{c_0}{c}\right)^2 \left[1 + i\frac{\alpha^{(\lambda)}}{27.29}\right], \tag{4}$$

where c and $\alpha^{(\lambda)}$, sound speed and absorption in dB/λ, are both functions of r and z.

In the absorption layer, squared index of refraction is given by

$$n^2 = \left(\frac{c_0}{c_b}\right)^2 + i\alpha \exp\left[-\left(\frac{z - z_{\max}}{D}\right)^2\right]. \tag{5}$$

where D is the width of the layer and α is generally 0.01. This gives an exponentially increasing absorption near the computational boundary.

2.5 Define Starting Field

For comparison with the Lloyd-mirror reference solution, the standard Gaussian source was included according to Eq. (6.101),

$$\psi(0, z) = \sqrt{k_0} e^{-\frac{k_0^2}{2}(z - z_z)^2}. \tag{6}$$

The boundary condition at the surface, $\psi(r, 0) = 0$ was included through an image source,

$$\psi(0.z) = \psi(0, z - z_s) - \psi(0, z + z_s).$$

For downslope propagation in a wedge (J&T, Fig. 1(a)), a line source with depth dependence of mode 3 placed in 100m water was used. Because this case was examined for only a qualitative comparison, an approximation of the line source was used instead:

$$\psi(0, z) = \begin{cases} \sin(\frac{3\pi}{100}z) + i\mathrm{sign}[\sin(\frac{3\pi}{100}z)] & 0 \leq z \leq 100, \\ 0 & z > 100, \end{cases} \tag{7}$$

which assumes a perfectly reflecting bottom boundary.

2.6 Choose Marching FFT Algorithm

By introducing the operators

$$A = \frac{ik_0}{2}[n^2(r, z) - 1]; \qquad B = \frac{i}{2k_0}\frac{\partial^2}{\partial z^2}, \tag{8}$$

the PE (1) may be written as a first-order differential equation

$$\partial\psi\partial r = (A+B)\psi = U(r,z)\psi. \tag{9}$$

The solution,

$$\begin{aligned} \psi(r,z) &= e^{\int_{r_0}^{r_0+\Delta r} U(r,z)dr}\psi(r_0,z) \\ &= \simeq e^{\widetilde{U}\Delta r}\psi(r_0,z) \end{aligned} \tag{10}$$

may be approximated with several different splittings of the exponential operator $e^{\widetilde{U}\Delta r}$.

The split-step marching solution recommended in the PE recipe in COA is derived from the exponential operator splitting

$$e^{(A+B)\Delta r} \simeq e^{A\Delta r}e^{B\Delta r}. \tag{11}$$

Its error is of order $(\Delta r)^2$. A different solution was used in the code, corresponding to the splitting

$$e^{(A+B)\Delta r} \simeq e^{\frac{A}{2}\Delta r}e^{B\Delta r}e^{\frac{A}{2}\Delta r}, \tag{12}$$

whose error is of order $(\Delta r)^3$. It is given by

$$\psi(r,z) = e^{\frac{ik_0}{4}[n^2(r_0,z)-1]\Delta r}\mathcal{F}^{-1}\Big\{e^{-\frac{i\Delta r}{2k_0}k_z^2}\mathcal{F}\Big\{e^{\frac{ik_0}{4}[n^2(r_0,z)-1]\Delta r}\psi(r_0,z)\Big\}\Big\} \tag{13}$$

This formulation is based on the form of the PE called the Tappert equation. Jensen and Tindle used the Thompson-Chapman equation. This code does not yet include the Thomson-Chapman equation.

2.7 Choose Numerical Fourier Transform

The derivation of the PE (1) assumes $\psi(r,0) = 0$. This boundary condition may be enforced through the use of the discrete Fast Sine Transform (FST) in (13). The FST assumes its input is a zero-point odd function, therefore, $\psi(r,0) = 0$. Complex values are easily handled by taking advantage of the linearity of Fourier Transforms,

$$\mathcal{F}\big\{x(t) + iy(t)\big\} = \mathcal{F}\big\{x(t)\big\} + i\mathcal{F}\big\{y(t)\big\}. \tag{14}$$

3 Numerical Results

3.1 Code Parameters

3.1.1 Physical Model, Lloyd Mirror Reference Solution

The reference solution for this code was the Lloyd-mirror interference pattern, where a point source is placed at a depth z_s, and an image source at $-z_s$ is used to enforce the boundary condition of $p(r,0)=0$. The equations are

$$p(r,z)=\frac{e^{ikR_1}}{R_1}-\frac{e^{ikR_2}}{R_2} \tag{15}$$

where

$$R_1=\sqrt{r^2+(z-z_s)^2}, \qquad R_2=\sqrt{r^2+(z+z_s)^2} \tag{16}$$

The physical environment is a simulated fluid half-space with sound speed $c=1500m/s$.

3.1.2 Physical Model, Downslope Propagation in a Wedge

The physical domain used by Jensen and Tindle is as follows:

- Ocean wedge: 10° slope, from depth 100m to 1863m.
- Physical Domain: 10 km in range, 2 km in depth.
- Water: $c_1 = 1500$ m s^{-1}, $\rho_1 = 1000$ kg m^{-3}, $\alpha = 0dB/\lambda$.
- Bottom: $c_2 = 1800$ m s^{-1}, $\rho_2 = 2000$ kg m^{-3}, $\alpha = 1dB/\lambda$.
- Source: f = 100 Hz, in 100 m water, line source with depth dependence of mode 3.

3.2 Comparison With Reference Solution

A comparison of the numerical results of the PE code and the analytical solution for the Lloyd-mirror pattern are shown in Figure (1).

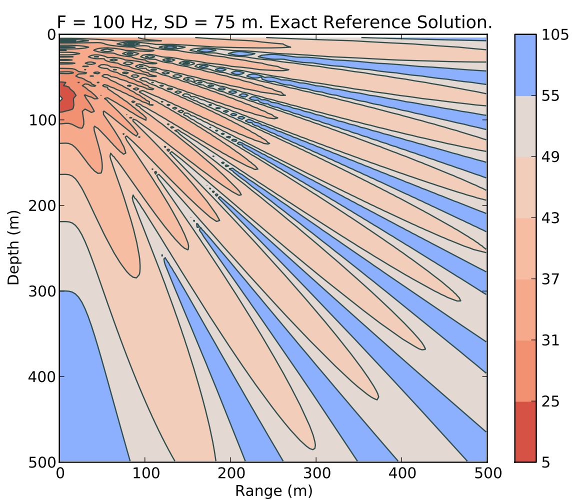

(a) Analytical Reference Solution, Transmission Loss

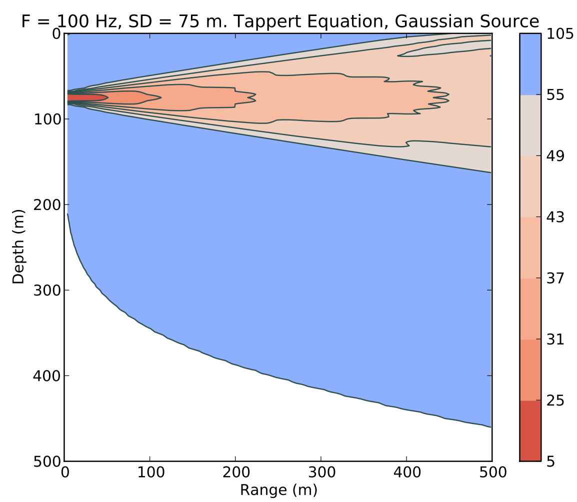

(b) Code Results,Transmission Loss

Figure 1

The code results are incorrect. An expansion of the computational domain range to 1500 m is shown in Figure (2).

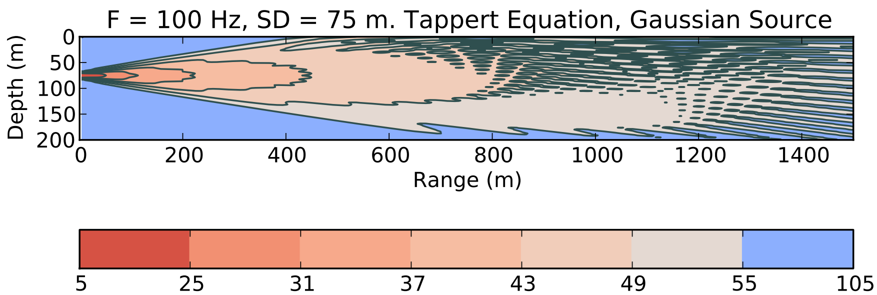

Figure 2: PE Code Results

It is apparent that the interference pattern is computed correctly but over the incorrect range scale. After a check of the inputs to the split-step marching algorithm and adjustment of parameters in order to localize the error, it was found that adding a factor of ten to the exponentials in Eq.(13) produced a qualitatively correct result, seen in Figure (3). This is equivalent to increasing the range step *within* the algorithm while mapping the results to the original range grid.

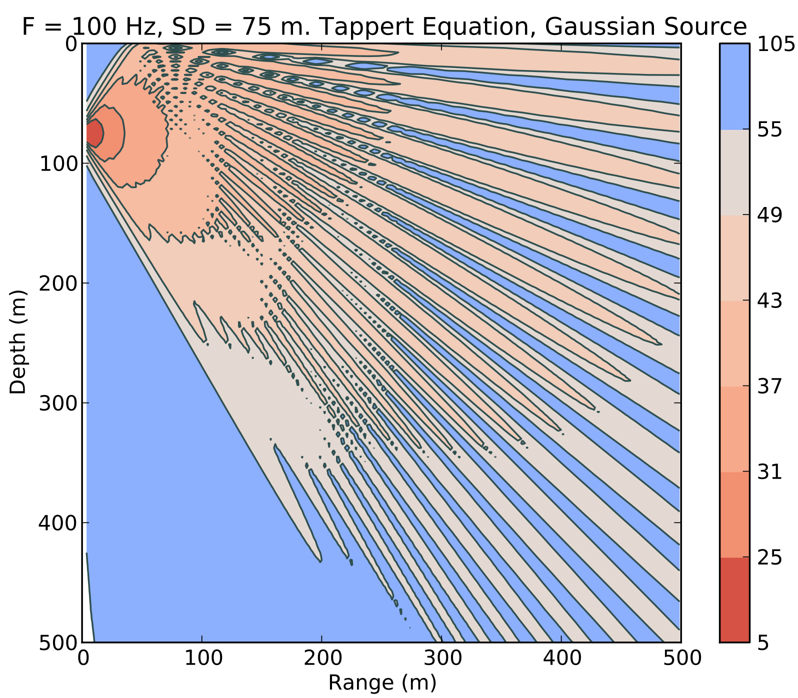

Figure 3: Adjusted PE Code Results

The difference between the reference solution and the ”corrected” results is shown in Figure (4). The large difference on the left hand side of the figure is to be expected as the Gaussian source has a limited angular aperture when compared to the point source. It may be possible to solve for the precise correction factor that would more accurately solve the Lloyd-mirror interference pattern. However, the correction factor, though useful at this time, would not be necessary once the true source of error is found.

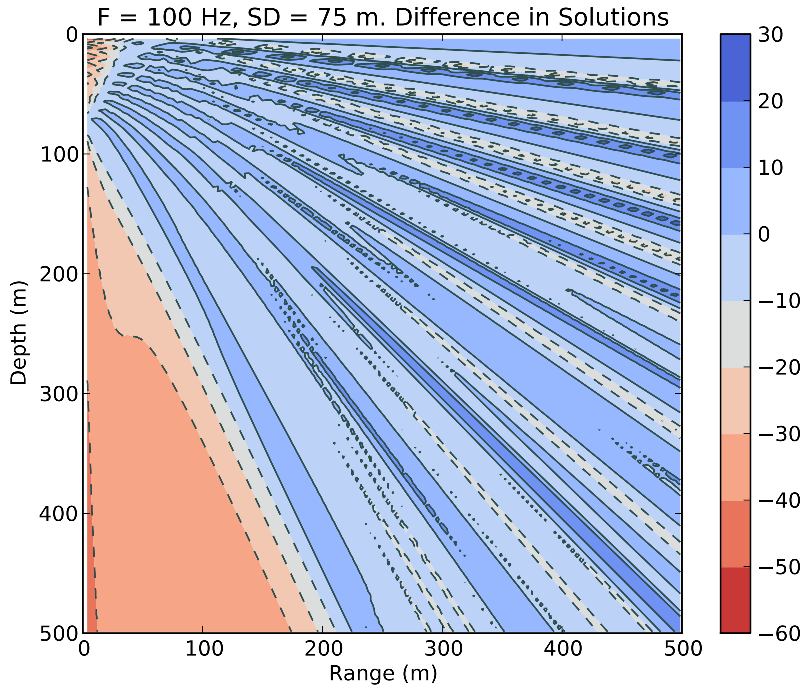

Figure 4: Difference Between Reference Solution and Code Results

3.3 Downslope Propagation in a Wedge

Code results were compared with Figure 1(a) of Jensen and Tindle (1987). The figure and code results are reproduced below.

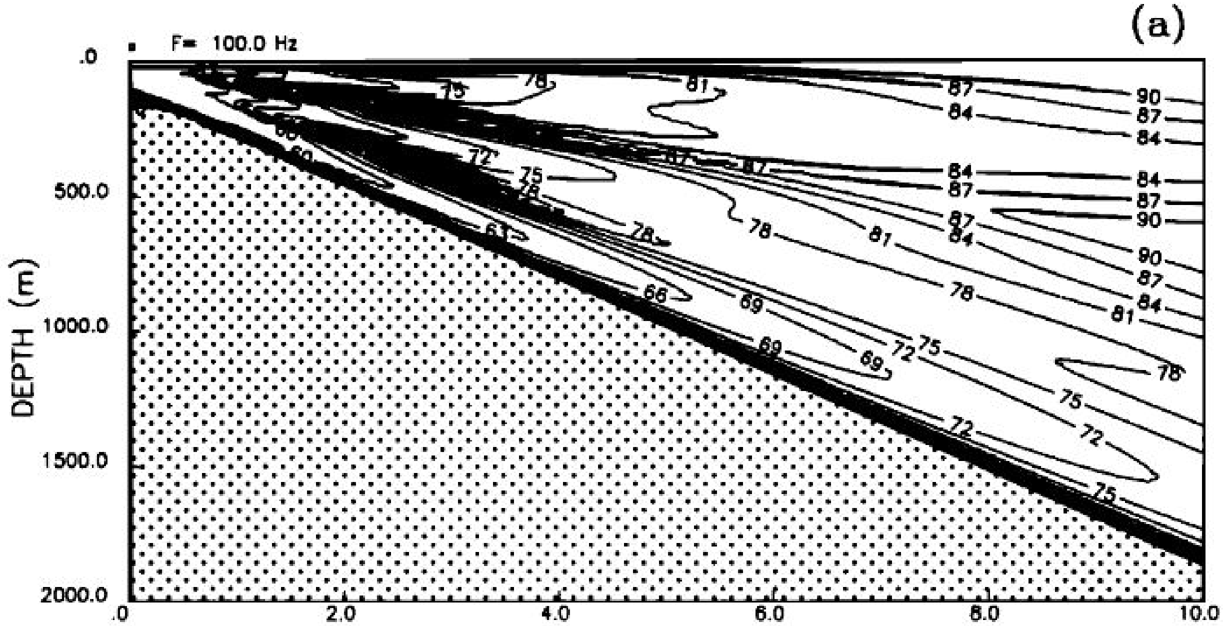

(a) Contours of dB loss for downslope propagation in a wedge. The source field has the depth dependence of mode 3 and simulates a vertical mode.

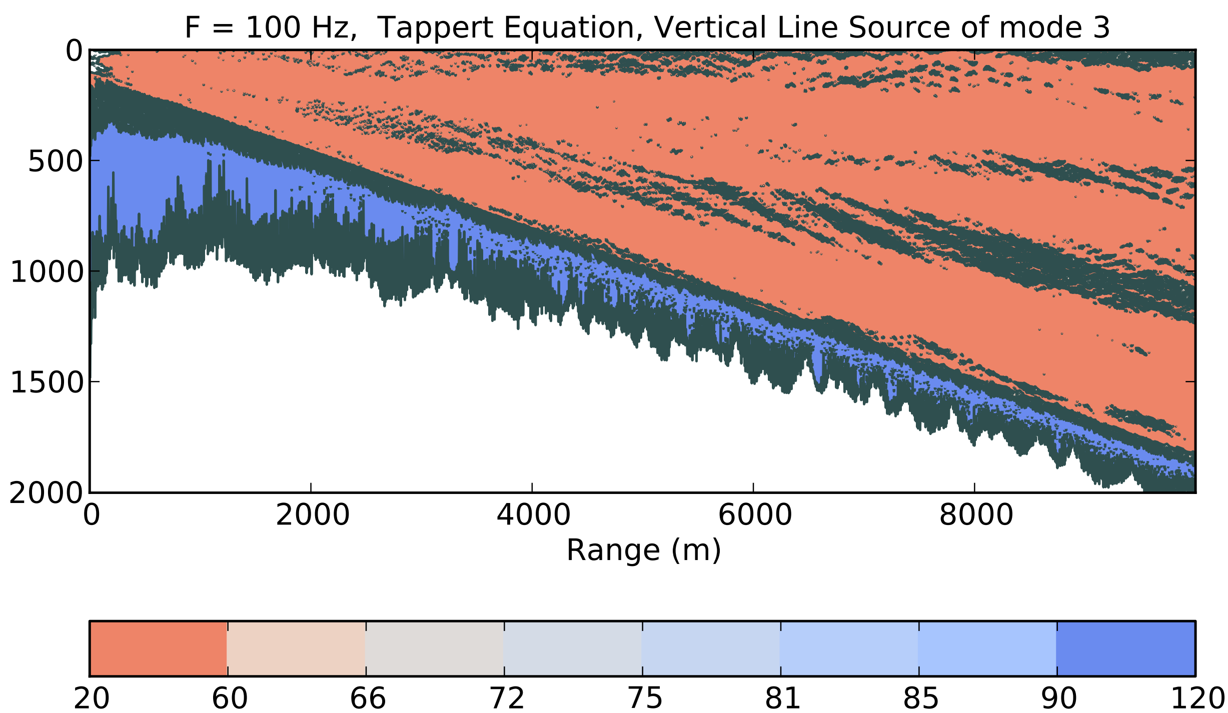

(b) Code Results, Contours of Transmission Loss

Figure 5

While similar to the published results, the code results are incorrect, due to the systematic error mentioned before. Some of the error is also certainly due to the approximation to the line source with depth dependence of mode 3 given by Eq. (7). As mentioned earlier, due to setbacks from the code error, upslope propagation was not examined.

4 Conclusion

A numerical PE code was developed and tested against a analytical reference solution. The code produces qualitatively correct results, and the error was isolated, but could not be fixed. It is written in MATLAB[3] and thus may be quickly adapted to a different physical environment. Once the error is found, this code could serve as an educational tool because, in contrast to other readily available PE codes, it is easy to read and does not require expertise in Fortran. The author plans to clone this code in the C programming language and then use the Python programming language to control it and plot the results.

[3]MATLAB is a registered trademark of The MathWorks, Inc.